Journal Pre-proof

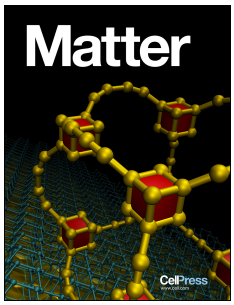

SARS-CoV-2 RapidPlex: A Graphene-based Multiplexed Telemedicine Platform for Rapid and Low-Cost COVID-19 Diagnosis and Monitoring

Rebeca M. Torrente-Rodríguez, Heather Lukas, Jiaobing Tu, Jihong Min, Yiran Yang, Changhao Xu, Harry B. Rossiter, Wei Gao

PII: S2590-2385(20)30553-1

DOI: https://doi.org/10.1016/j.matt.2020.09.027

Reference: MATT 460

To appear in: *Matter*

Received Date: 1 September 2020

Revised Date: 20 September 2020

Accepted Date: 29 September 2020

Please cite this article as: Torrente-Rodríguez RM, Lukas H, Tu J, Min J, Yang Y, Xu C, Rossiter HB, Gao W, SARS-CoV-2 RapidPlex: A Graphene-based Multiplexed Telemedicine Platform for Rapid and Low-Cost COVID-19 Diagnosis and Monitoring, *Matter* (2020), doi: https://doi.org/10.1016/j.matt.2020.09.027.

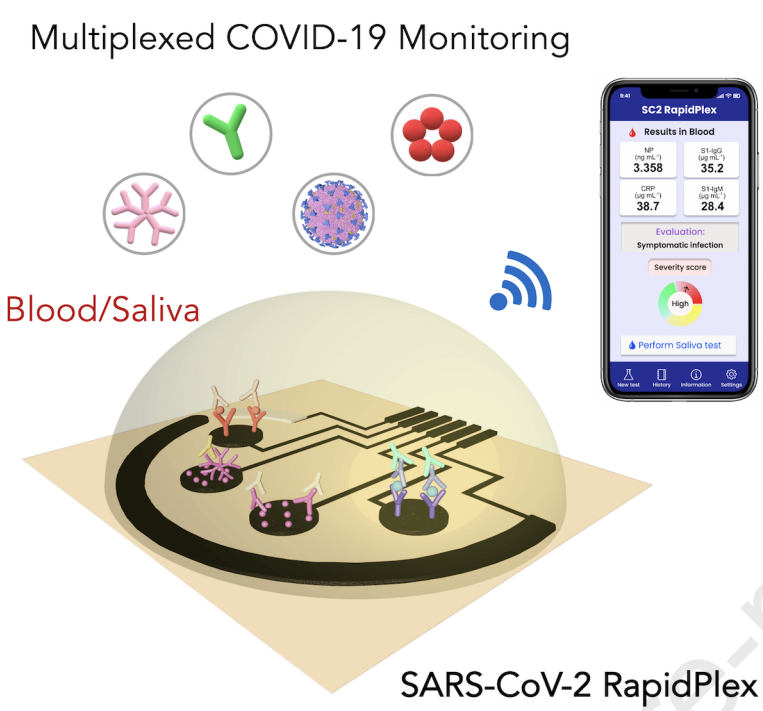

SARS-CoV-2 RapidPlex: A Graphene-based Multiplexed Telemedicine Platform for Rapid and Low-Cost COVID-19 Diagnosis and Monitoring

Rebeca M. Torrente-Rodríguez,[1,3] Heather Lukas,[1,3] Jiaobing Tu,[1] Jihong Min,[1] Yiran Yang,[1] Changhao Xu,[1] Harry B. Rossiter,[2] Wei Gao[1,4,*]

[1]Andrew and Peggy Cherng Department of Medical Engineering, California Institute of Technology, Pasadena, California, 91125, USA

[2]Rehabilitation Clinical Trials Center, Division of Respiratory and Critical Care Physiology and Medicine, The Lundquist Institute for Biomedical Innovation at Harbor-UCLA Medical Center, Torrance, California, 90502, USA

[3]These authors contributed equally to this work

[4]Lead contact

*Email: weigao@caltech.edu

SUMMARY

The COVID-19 pandemic is an ongoing global challenge for public health systems. Ultrasensitive and early identification of infection is critical to prevent widespread COVID-19 infection by presymptomatic and asymptomatic individuals, especially in the community and in-home settings. We demonstrate a multiplexed, portable, wireless electrochemical platform for ultra-rapid detection of COVID-19: the SARS-CoV-2 RapidPlex. It detects viral antigen nucleocapsid protein, IgM and IgG antibodies, as well as the inflammatory biomarker C-reactive protein, based on our mass-producible laser-engraved graphene electrodes. We demonstrate ultrasensitive, highly selective, and rapid electrochemical detection in the physiologically relevant ranges. We successfully evaluated the applicability of our SARS-CoV-2 RapidPlex platform with COVID-19 positive and negative blood and saliva samples. Based on this pilot study, our multiplexed immunosensor platform may allow for high frequency at-home testing for COVID-19 telemedicine diagnosis and monitoring.

INTRODUCTION

On March 11, 2020, the World Health Organization characterized the COVID-19 outbreak as a pandemic. Six months later, the global health crisis had continued with over 30 million confirmed cases of novel coronavirus globally – over 22% of these were in the United States.[1] It is estimated that 14-20% of patients will develop severe illness requiring hospitalization.[2] Initial efforts to mitigate the spread through state-mandated "stay-at-home" orders appeared effective, however, reopening of the US economy resulted in renewed exponential spread of novel coronavirus, as predicted.[3] It is estimated that the US GDP will suffer losses upwards of $45.3 billion during a flu-like pandemic without available vaccines.[4] Safe reopening of the economy, schools and universities requires multiple approaches to mitigate the risks associated with COVID-19, including simple, affordable and effective test-and-trace measures.

Containing the spread is difficult due to the challenges in identifying infectious individuals. Most COVID-19 community spread may occur in the absence of symptoms. Peak viremia may be at the end of the incubation period, allowing for a transmission-sufficient viral load 1-2 days prior to symptom onset.[3] Additionally, due to the unknown duration and prevalence of asymptomatic cases, the true reproduction number may be under-estimated.[5,6] Reported incidence of asymptomatic patients ranges from 17.9% to 30.8%.[7,8]

Increased access to COVID-19 testing has allowed increased monitoring of the community spread, but several diagnostic challenges remain. Currently, the standard testing method is viral nucleic acid real-time polymerase chain reaction (RT-PCR), which is a slow process[9] and requires expensive equipment and trained technicians for nasopharyngeal swab sample collection and analysis.[9] In addition, the sheer volume of testing required is overwhelming the ability for healthcare systems to report RT-PCR results to patients, causing, in some states, delays of ~7-10 days to inform positive[10] findings and enact isolation and monitoring protocols. Despite the recent advances on point-of-care (POC) rapid RT-PCR test,[11–15] nucleic acid tests are also known to produce false negatives, which may limit containment strategies and access to treatment.[16] An additional consideration for RT-PCR is that it only identifies active carriers of the virus. Identifying convalescent persons based on COVID-19 antibody presentation is equally important as it may provide health officials with crucial information regarding the potential impact of reopening measures.[17] Serologic assays detect circulating antibodies specific to SARS-CoV-2 antigens, including the nucleocapsid

protein and the outer spike protein.[9,18] However, it is not possible to differentiate between asymptomatic carriers and immune persons using antibody detection. Therefore, to effectively mitigate the risks of COVID-19 community spread, systems are required that determine simultaneously both the viral and serologic status of an individual. Moreover, recent studies show correlation between circulating inflammatory biomarker concentration and COVID-19 severity.[19] Increased C-reactive protein (CRP) concentration is found in patients diagnosed with COVID-19 pneumonia and is associated with increasing severity, suggesting a role in diagnosis and prognosis of COVID-19 patients.[20,21]

There is a clear and urgent need for a highly sensitive, rapid, inexpensive, telemedicine COVID-19 test that can identify a patient's past and present infection status.[22] There has been progress towards POC COVID-19 testing, but all commercially available test kits provide only qualitative results. Quantitative analysis of COVID-19 biomarkers using a telemedicine device may provide predictive information of disease severity and provide seroconversion information regarding disease time course. Electrochemical biosensors, in this regard, are advantageous due to their rapid detection efficacy and ease of use for POC applications.[23–27] Simple, safe and effective COVID-19 sample collection has proved challenging given current assay requirements. Saliva-compatible POC assays would be advantageous since saliva contains rich information and can be easily and non-invasively collected by patients themselves for telemedicine testing.[28]

Here, we present a novel multiplexed, portable, wireless electrochemical platform for ultra-rapid detection of COVID-19: SARS-CoV-2 RapidPlex (**Figure 1**). This platform quantitatively detects biomarkers specific to COVID-19 in both blood and saliva including SARS-CoV-2 nucleocapsid protein (NP), specific immunoglobulins (Igs) against SARS-CoV-2 spike protein (S1) (S1-IgM and S1-IgG), and CRP, within physiologically relevant ranges. The platform uses capture antigens and antibodies immobilized on mass-producible, low-cost laser-engraved graphene (LEG)[29,30] electrodes. This multiplexed platform tracks the infection progression by diagnosing the stage of the disease, allowing for the clear identification of individuals who are infectious, vulnerable, and/or immune (**Table 1**). The main features of SARS-CoV-2 RapidPlex are high sensitivity, low cost, ultra-fast detection, wireless remote and multiplexed sensing that provides information on three key aspects of COVID-19 disease: viral infection (NP),[31] immune response (IgG and IgM),[9] and disease severity (CRP).[19–21]

RESULTS AND DISCUSSION

Design of the SARS-CoV-2 RapidPlex Platform

As illustrated in **Figure 1A**, SARS-CoV-2 RapidPlex is composed of four graphene working electrodes (WEs), a Ag/AgCl reference electrode (RE), and a graphene counter electrode (CE), all of them patterned on a polyimide (PI) substrate via CO_2 laser engraving, a fast, high-throughput, and cost-effective production method (**Figure 1B** and **1C**). Our group has recently demonstrated the use of mesoporous graphene structure fabricated by laser engraving for high performance and low-cost biosensing.[29,30] The materials cost for the unmodified RapidPlex platform is within $0.05; additional chemical and reagent costs for the multiplexed sensor preparation are at the level of dollars depending on the order sizes. Detection of selected target proteins (NP and CRP) and specific immunoglobulins (S1-IgG and S1-IgM) is achieved through sandwich- and indirect-based immunosensing strategies onto the LEG electrodes, respectively. The superior properties of graphene, in terms of high charge mobility and surface area together with the high sensitivity and selectivity of sensing strategies involving both capture and detector receptors, make our device (**Figure 1D**) a highly convenient tool for the rapid, accurate, and stage-specific COVID-19 infection detection in blood as well as in non-invasive biofluid samples, such as saliva.

Electrochemical Characterization of SARS-CoV-2 RapidPlex Platform

Functionalization and modification steps carried out on the LEG surfaces for the covalent attachment of each of the specific receptors required for the development of our SARS-CoV-2 RapidPlex platform is schematized in **Figure 2A**. 1-pyrenebutyric acid (PBA) is used as the linker to anchor the required receptors to the graphene layer. Although attachment of functional groups directly on the sp^2 carbon atom surface is one of the common ways to functionalize graphene, these methods are associated with the requirement of defects or edges in the sensor material, which could alter its specific physical properties.[32,33] In contrast, introduction of functional groups on the sensing layer by means of pyrene derivatives is preferred here as it does not disrupt the conjugation of the graphene sheets and improves its stability.[34,35] PBA consisting of a pyrene group that contains π-electrons and a carboxylic group is used to functionalize graphene layers via π-stacking and hydrophobic interactions. The pyrene units of PBA strongly interact with graphene layers in the way that original structure and properties of the graphene are well maintained. The functional moieties contained in each PBA molecule allow the preparation of the affinity-based biosensing platform through the covalent coupling between the carboxylic groups on PBA units and the

–NH_2 groups of the respective capture receptors (specific antibodies or capture proteins). Blocking of unreacted sites with bovine serum albumin (BSA) impedes the non-specific adsorption of other molecules involved in each assay configuration or circulating in the sample of interest.

Differential pulse voltammetry (DPV) and open circuit potential-electrochemical impedance spectroscopy (OCP-EIS) techniques are employed to electrochemically characterize and prove the stepwise self-assembled processes in both assay configurations for the detection of selected target molecules. DPV readings reflect lower peak current intensity after each modification step related to S1-Ig assay due to the hindered diffusion of the redox label to the electrode surface derived from both the carboxyl groups and the attached proteins and biological macromolecules (**Figure 2B**). At the same time, resistance in the Nyquist plots from OCP-EIS is increased after each functionalization step (**Figure 2C**). The successful anchorage of PBA was also verified with scanning electron microscopy (SEM) (**Figure S1**). Electrochemical characterization of the sandwich assay-based sensor modification using CRP protein as a model molecule and the aforementioned techniques are presented in **Figure S2**.

To preserve the native structure and properties of the bound biomolecules, PBA was chosen as a heterobifunctional linker, effectively preventing the direct interaction between large biomolecules and the graphene surface.[33] In order to verify this selection, CRP and SARS-CoV-2 specific IgG assay configurations were constructed on graphene electrodes functionalized with PBA and another common linker, 1H-pyrrole-1-propionic acid (PPA).[30] Greater signal-to-blank (S/B) ratios were observed for both assays where PBA was used as a linker support (**Figure 2D**), mainly due to a significant decrease in the signals obtained in the absence of the corresponding target molecule when PBA was used instead of PPA. Together with an optimal blocking strategy, PBA can be used for the immobilization of specific biomolecular probes (e.g. antibodies, proteins, etc.) while avoiding non-specific adsorptions in the context of immunoassays.[36]

The orientation of modified antigenic proteins on solid surfaces is strongly associated with their activity and reactivity. Specific anti-His antibodies can be used to orient the immobilization of antigenic receptors containing histidine residues, but this implies an additional step compared with their direct attachment on the sensing layer, as it is schematized in **Figure S3A**. Our results show no significant differences in assay performance for IgG detection on PBA-graphene electrodes covalently functionalized with the specific

coating protein (direct immobilization) and with anti-His antibodies for the previous capture of the polyhistidine-tag specific coating protein (oriented immobilization) (**Figure S3B**), proving that random protein orientation does not interfere with the epitope accessibility for effective recognition by specific target antibodies. This is in agreement with other reports confirming that His-tagged fusion antigens can be directly immobilized on different surfaces with protein orientations completely compatible with antibody recognition.[37–40] In order to simplify and reduce the cost and time of the assay, direct immobilization of S1 protein was carried out for specific Ig detection.

Considering that rapid target binding is essential to the successful implementation of our proposed platform as a POC system, we investigated how target (or sample) incubation time affects the response of each biosensor comprising our SARS-CoV-2 RapidPlex platform. **Figure 2E** summarizes the amperometric signals obtained for each of the four sensing units at different incubation times (1, 5 and 10 minutes) in the absence (blank, B) and in the presence (S) of 500 pg mL^{-1}, 250 ng mL^{-1}, and 50 ng mL^{-1} of NP, SARS-CoV-2 specific IgG and IgM isotypes, and CRP, respectively. It is important to note that although a 10-minute incubation time was selected for most of the studies here in order to ensure the highest sensitivity for the determination of ultra-low levels of each target molecule, a significant difference between the absence and the presence of each of the corresponding targets is obtained with just 1-minute incubation time. This provides one of the major advantages of our SARS-CoV-2 RapidPlex system as a rapid POC device for SARS-CoV-2 infection monitoring with the required sensitivity for both protein and Ig determination. ELISA,[17,41–44] nucleic acid amplification,[45–49] mass spectrometry,[50] or even combinations[51] have been reported very recently for determination of the proposed SARS-CoV-2 specific target molecules, among others. However, most of these methods show crucial pitfalls, mainly in terms of sample preparation, complexity, and expensive and bulky equipment requirements, that make them still highly difficult to be implemented as POC systems. Our device provides an attractive alternative to standard assays for protein determination, such as ELISA, because of its multiplexing capabilities, remote functionality and short sample-to-answer time.

Evaluation of Analytical Performance of the SARS-CoV-2 RapidPlex

The performance of each biosensor contained in the SARS-CoV-2 RapidPlex was characterized in phosphate-buffered saline (PBS) solutions supplemented with 1.0% of bovine serum albumin (BSA) by measuring the amperometric readout in the presence of

increased concentrations of NP, S1-IgG, S1-IgM, and CRP (**Figure 3**). The selected strategies for NP viral antigen and CRP proteins are based on double sandwich and sandwich configurations, respectively, as illustrated in **Figure 3A**. The sandwich-based immunoassays for antigen detection are, in general, highly sensitive due to the involvement of two different antibodies as capture and detector entities. According to the low levels that must be reached for NP and CRP in diluted serum and saliva (pg mL^{-1} to ng mL^{-1}), we think these strategies are the most suitable to be implemented on our platform. Variation of cathodic currents with the concentration for NP and CRP in buffered solutions are presented in **Figure 3B** and **3C**, respectively. S1-IgG and S1-IgM were detected based on indirect immunoassays (**Figure 3D**), which are considered highly suitable for detection of circulating macromolecules in antisera and other biofluids. **Figure 3E** and **3F** show the calibration curves for S1 specific Ig determination (S1-IgG and S1-IgM, respectively) in buffered solutions. Reproducibility was demonstrated through the relative standard deviation (RSD) values obtained with different biosensors prepared in the same manner on different days. RSD values of 6.3%, 8.4%, 6.0% and 7.6% for 20 ng mL^{-1} CRP, 250 ng mL^{-1} S1-IgG, 250 ng mL^{-1} S1-IgM and 500 pg mL^{-1} NP antigen (n=5) demonstrate good reproducibility in both device preparation and signal transduction. In addition, the sensors showed stable responses over a 5-day storage period at 4 °C (**Figure S5**). We did not observe significant slope variations between data obtained in properly diluted human serum and in buffered solutions for the determination of each target analyte (for instance, the slope sensitivity value (16.28 nA mL ng^{-1}) obtained for CRP as model analyte in PBS buffered solutions is nearly the same as that in diluted serum samples from a healthy volunteer (16.64 nA mL ng^{-1})); therefore, accurate quantification of the proposed target analytes can be carried out by conducting a simple interpolation of the cathodic readings obtained for each sample tested in the corresponding calibration curve constructed in buffered solution.

Since diagnostic sensitivity and specificity of seroprevalence studies can be improved by using a mixture of antigenic proteins instead of a single protein,[52,53] we modified graphene with a mixture of SARS-CoV-2 related antigens, NP and S1, to capture specific immunoglobulin isotypes against both antigens in the same WE. A calibration curve for (NP + S1)-IgG detection is shown in **Figure S4**. Thus, this methodology can be tailored for detecting isotype-specific IgG (or IgM) or a combination of both Ig isotypes in the same sensing surface to better capture total Ig concentration and thus increase assay sensitivity across the patient population.

Investigation of the Selectivity and Multiplexed Performance of the SARS-CoV-2 RapidPlex

Human biofluids contain a complex and variable mixture of circulating molecules that could interfere with molecular sensing. In addition, negligible crosstalk between different working surfaces is an essential requirement to perform multiplexed detection readings accurately and meaningfully. Therefore, selectivity and crosstalk of the SARS-CoV-2 RapidPlex platform were evaluated. Amperometric readings obtained for each developed biosensor against non-target molecules are presented in **Figure 4A**. We evaluated the specific binding for SARS-CoV-2 biomarkers in comparison to biomarkers of similar coronaviruses, including SARS-CoV and MERS-CoV. We observed no significant cross-reaction for NP, S1-IgG, S1-IgM and CRP assays in the presence of each tested interferent, including SARS-CoV-2 S1, SARS-CoV S1, and CRP (for NP assay), SARS-CoV-2 NP-IgG, SARS-CoV IgG, MERS-CoV IgG, S1-IgG, and negative controls containing mixtures of IgG and IgM against both MERS-CoV and SARS-CoV (for S1-IgG and S1-IgM assays), and BNP, NP, SARS-CoV NP and SARS-CoV S1 (for CRP assay), respectively. However, SARS-CoV NP viral antigen interferent provided a cathodic current corresponding to ~80% of the raw current obtained for the detection of the specific NP antigen. Spike, envelope, and membrane SARS-CoV-2 proteins share 76-95% sequence identity with those of SARS-CoV. This percentage homology is reduced to 30-40% for MERS-CoV. Similarly, since SARS-CoV-2 NP is 90% identical to SARS-CoV NP,[17,54–56] the interference observed from SARS-CoV NP antigen was expected. However, the lack of selectivity in this particular case is not a major concern due to the absence of new SARS-CoV cases detected recently; therefore, it can be inferred that this interference will not produce a barrier for selective SARS-CoV-2 NP determination in real samples. We further evaluated the amperometric-derived concentrations with absorbance-derived concentrations collected via ELISA. As it is presented in **Figure 4B**, the results from our functionalized electrochemical biosensor were linearly correlated ($r = 0.955$) with the results using the same reagents in a traditional ELISA protocol.

Once the performance and selectivity of each constructed biosensor was individually and exhaustively evaluated, we demonstrate the multiplexing capabilities of our four-working-electrode (4WEs) graphene array device designed with a Ag/AgCl RE and a graphene CE. The block diagram showing the functional units that comprise the integrated electronic system is illustrated in **Figure 4C** and **4D**. Amperometric readings from the four channels are concurrently taken and data is wirelessly transmitted to a user device over Bluetooth Low

Energy. The electronic system, including the printed circuit board (PCB) and a lithium-ion polymer battery, is 20 × 35 × 7.3 mm in dimension. The compact device can perform amperometric measurements continuously for over 5 hours in a single charge.

With the objective of demonstrating the utility of our SARS-CoV-2 RapidPlex array for multiplexed and simultaneous quantification of selected target molecules, we evaluated the potential cross-reaction resulting from the diffusion of signal substances between adjacent immunosurfaces. For this, each of the four conveniently functionalized working surfaces were incubated with buffered solutions containing significantly high concentration of each of the selected targets, followed by the corresponding detector receptors in each case. The absence of cross-talk between the adjacent working electrodes is verified from the experimental readings in buffered solutions containing 1.0 ng mL^{-1} NP antigen (I), 250 ng mL^{-1} S1 specific IgG (II) and -IgM (III), and 50 ng mL^{-1} CRP (IV) (**Figure 4E**). As envisaged, significantly higher signal was obtained when each target was specifically captured and further labeled by its tracer antibody in the corresponding functionalized immunosurface. These results, in conjunction with those from **Figure 4A** demonstrate the feasibility of the developed SARS-CoV-2 RapidPlex platform for fast, selective and reliable determination of NP, S1-IgG and S1-IgM isotypes, and CRP in one single experiment. It should be noted that since IgG and IgM have similar binding mechanisms to viral antigens and individual quantification of Igs require no mixing of the specific detector labels, individual droplets were used on IgG and IgM sensing electrodes during modification and labelling.

Detection of SARS-CoV-2 Related Selected Targets in Human Biospecimens

To prove the utility of our device in a more complex and real scenario, we evaluated the multiplexed capabilities of SARS-CoV-2 RapidPlex in representative serum samples from COVID-19 RT-PCR negative and positive subjects. Sensor data from the serum samples of a RT-PCR negative subject (**Figure 5A**) and a RT-PCR positive patient (**Figure 5B**) show minimal cross-talk in a real and complex sample matrix, indicating the efficient functionality of SARS-CoV-2 RapidPlex to simultaneously differentiate the overexpressed presence of SARS-CoV-2 related target reporters in COVID-19 positive specimens. Moreover, the SARS-CoV-2 RapidPlex device is able to provide significant positive readings for all targets after incubating the COVID-19 positive serum sample for just 1 minute (**Figure 5C** and **Figure S5**): The maintained high signal in positive patient samples demonstrates the great

potential in future translation of the SARS-CoV-2 RapidPlex device as an ultra-fast POC remote diagnostic tool.

To further investigate NP, S1-IgG, S1-IgM, and CRP response to SARS-CoV-2 infection using our LEG-based biosensors, each target molecule was measured in serum and saliva samples from RT-PCR confirmed COVID-19 positive and negative subjects. Obtained results were plotted as the ratio between the amperometric readings for each sample tested (S) and the respective blank (B) in each case to compare target detection in different concentration ranges. Using the graphene sensors, a total of 17 COVID-19 RT-PCR tested serum samples (10 positive, 7 negative) were assayed, and a total of 8 COVID-19 RT-PCR tested saliva samples (5 positive, 3 negative) were analyzed (**Table S1**).

Results from **Figure 5D** and **5E** corroborate that, as expected, compared to RT-PCR negative subjects, RT-PCR positive COVID-19 patients show significantly elevated levels of the selected targets in both serum and saliva samples, with median S/B ratios of 10.53, 11.62, 10.67 and 12.39 in serum, and 2.81, 3.24, 1.62, and 1.76 in saliva, for NP, S1-IgG, S1-IgM, and CRP, respectively. We observed a concentration of NP in the range of 0.1-0.8 μg mL^{-1} and 0.5–2.0 ng mL^{-1} in COVID-19 patient serum and saliva, respectively; S1-IgG in the range of 20–40 μg mL^{-1} and 0.2–0.5 μg mL^{-1} in COVID-19 patient serum and saliva, respectively; S1-IgM in the range of 20–50 μg mL^{-1} and 0.6–5.0 μg mL^{-1} in COVID-19 patient serum and saliva, respectively; and CRP in the range of 10–20 μg mL^{-1} and 0.1–0.5 μg mL^{-1} in COVID-19 patient serum and saliva, respectively. The factor that all the positive samples show much higher signals compared to negative samples proves the real utility for the accurate evaluation of the COVID-19 biomarkers in biofluids using our LEG-based biosensors. In particular, the observed significant presence of COVID-19 biomarkers in saliva demonstrates the great utility of this biofluid as a valuable source for non-invasively diagnosing and monitoring SARS-CoV-2 infection.

With the aim to confirm the relationship between the levels of inflammatory biomarkers involved in the cytokine storm directly associated with disease progression, severity and outcome in COVID-19,[57–62] we evaluated the variation of serum CRP levels in RT-PCR negative subjects (n=7) and RT-PCR positive COVID-19 patients who were classified clinically according to disease severity as asymptomatic (n=2), mild (n=5), moderate (n=2). As shown in **Figure 5F**, we observed a positive association between CRP concentration and COVID-19 symptom severity grade, consistent with the recent literature reports.[20,61] Future

clinical testing using paired saliva and serum samples over the course of the infection is required to determine the relationship between saliva and serum concentrations and validate the utility of our platform in identifying severity-specific COVID-19 (**Table 1**).

CONCLUSIONS

To address the increasing demands for effective diagnostic tools for simple COVID-19 detection with immediate sample-to-answer turnaround, we have developed and implemented the first multiplexed electrochemical graphene-based platform, SARS-CoV-2 RapidPlex, for sensitive, rapid and selective simultaneous interrogation of NP viral antigen, S1-IgG and -IgM isotypes, and CRP in serum and saliva biofluids from healthy and RT-PCR confirmed COVID-19 infected patients. The combination of the advantageous properties of graphene material with the high sensitivity and specificity of the immunosensing strategies makes our SARS-CoV-2 RapidPlex platform a promising diagnostic device for the accurate monitoring of COVID-19 infection in serum and non-invasively accessible body fluids free from complex sample pretreatment requirements. Due to the ease of use, saliva sample compatibility, and rapid time to results, the SARS-CoV-2 RapidPlex platform has high potential for implementation at POC for patient triage, as well as for at-home use for telemedicine care and remote monitoring.

Monitoring of selected targets in one single and fast experiment (target capture can be as low as 1 minute) provides substantial information not only regarding early COVID-19 infection through viral antigen and IgM isotype detection, but also about disease severity by means of CRP evaluation and potential acquired immunity through IgG isotype quantification. The rapid on-site evaluation of disease severity enabled by our SARS-CoV-2 RapidPlex introduces the unparalleled advantage of immediate COVID-19 triaging. In future clinical applications, this could not only alert attending physicians of cases requiring major and careful medical attention but also facilitate the efficient allocation of precious medical resources, such as ventilators and ICU beds, in the event of resurging outbreaks to optimize patient outcomes under an overloading of local healthcare systems.

Our proposed methodologies based on simple, yet well-established surface functionalization techniques and sensing principles allow the ease of translation to the detection of other highly informative SARS-CoV-2 related reporters just by simply changing the coating capture receptor. Further technological improvement could be achieved by introducing fully automated sample handling process through a microfluidic module for telemedicine

deployment. Modification of our platform design may allow for rapid viral antigen and antibody panel testing such that COVID-19 infection could be clearly distinguished from non-specific symptoms of seasonal respiratory infections, such as influenza. Additionally, the wireless telemedicine diagnostic platform when coupled with emerging wearable biosensors to continuously monitor vital signs and other chemical biomarkers could provide comprehensive information on an individual's health status during the COVID-19 pandemic.[63–67]

Our platform pioneers multiplexed detection of stage-specific SARS-CoV-2 related biomarkers to provide a detailed and personalized snapshot of the COVID-19 infection. We firmly believe that our developed platform will be a high utility testing method towards fighting this and future pandemics, helping to end one of the deepest global health, economic and humanitarian crises in modern history.

EXPERIMENTAL PROCEDURES

Resource Availability

Lead Contact

Further information and requests for materials should be directed to and will be fulfilled by the Lead Contact, Wei Gao, weigao@caltech.edu.

Materials Availability

The materials generated in this study are available from the corresponding author upon request.

Data and Code Availability

The data used to support the findings of this study are available from the corresponding author upon request.

Materials and Reagents

1-Pyrenebutyric acid (PBA, 97%), 1H-pyrrole-1-propionic acid (PPA, 97%), 1-ethyl-3-(3-dimethylamonipropyl)carbodiimide (EDC), N-hydroxysulfosuccinimide (Sulfo-NHS), bovine serum albumin (BSA), hydroquinone (HQ), 2-(N-morpholino)ethanesulfonic acid hydrate (MES), Tween® 20, sodium thiosulfate, sodium bisulfite and potassium ferrocyanide (II) were purchased from Sigma Aldrich. Streptavidin-POD conjugate (Streptavidin-HRP,

11089153001) was purchased from Roche. Sodium dihydrogen phosphate, potassium hydrogen phosphate, potassium chloride, hydrogen peroxide (30% w/v), sulfuric acid and flat-bottom NUNC^{TM} 96-well microplates were purchased from Fisher Scientific. Potassium ferricyanide (III) and silver nitrate, iron (III) chloride and 0.1 M PBS (pH 7.4) were purchased from Across Organics and Alfa Aesar, respectively. N,N-Dimethylformaide (DMF) and Isopropyl alcohol (IPA) were purchased from Fisher Chemical and VWR Chemicals respectively. Anti-CRP murine monoclonal antibody and human CRP standard were purchased from R&D Systems (DY1707). CRP polyclonal antibody labeled with HRP (PA1-28329) and 3,3',5,5' tetramethylbenzidine (TMB) colorimetric substrate was purchased from Invitrogen. Mouse nucleocapsid protein (NP) monoclonal antibody (40143-MM05), SARS-CoV-2 NP antigen (40588-V08B), SARS-CoV/SARS-CoV-2 nucleocapsid antibody, rabbit mAb (40143-R001), SARS-CoV NP antigen (HCoV-OC43; 40643-V07E), SARS-CoV-2 Spike S1-His Recombinant Protein (HPLC-verified) (40591-V08H) and SARS-CoV Spike S1 Protein (S1 Subunit, His Tag) (40150-V08B1) were purchased from Sino Biological. His-tagged SARS-CoV-2 Spike S1 protein (PNA002), His-Tagged SARS-CoV-2 Nucleocapsid protein (PNA006), anti-Spike-RBD fully human mAb (IgG) (S1-IgG, AHA013), anti-NP mAb (IgG) (SARS-CoV-2 NP-IgG, AHA009), SARS-CoV antibody-80R (IgG) (CHA001) and MERS-CoV antibody-2E6 (IgG) (CHA002) were purchased from Sanyou Bio. Rabbit anti-human IgG IgG H&L (HRP) (ab6759), recombinant human BNP (ab87200), rabbit anti-human IgM mu chain (HRP) (ab97210), goat anti-rabbit IgG H&L (HRP) (ab97051), and rabbit polyclonal anti-6X His tag antibody (ab9108) were purchased from Abcam. Human Spike-SARS-CoV-2 IgM (S1-IgM, MBS2614311) were purchased from MyBiosource. MERS-CoV/SARS-CoV negative control (CI 2601-0101 Z) was purchased from Euroimmun. Polyimide film (PI, 125 µm thick) was purchased from DuPont.

Fabrication of Multiplex Array Electrode

For four channel graphene sensor fabrication, a PI film was attached onto a supporting substrate in a 50 W CO_2 laser cutter (Universal Laser System VLS3.50). Selected laser-cutting parameters were: Power 8.0%, Speed 15%, Points Per Inch (PPI) 1000, in raster mode and at focused height. Ag/AgCl reference electrodes (RE) were fabricated by electrodeposition in 40 µL of a mixture solution containing silver nitrate, sodium thiosulfate, and sodium bisulfite (final concentrations 250 mM, 750 mM and 500 mM, respectively) for 100 seconds at -0.2 mA, followed by drop-casting 20 µL-aliquot of $FeCl_3$ for 1 minute.

Functionalization of the SARS-CoV-2 RapidPlex and Electrochemical Readout

10 µL-aliquot of 5.0 mM PBA in DMF was drop-casted on the graphene surface and incubated for 2 hours at room temperature in a humid chamber. After rinsing with DMF, IPA, deionized (DI) water and drying under air flow, electrodes were incubated with 10 µL of a mixture solution containing 0.4 M EDC and 0.1 M Sulfo-NHS in 0.025 M MES (pH 6.5) for 35 minutes at room temperature under humid ambient conditions. Specific antibodies or coating protein were covalently attached onto activated surface by drop-casting 5.0 µL of the specific reagent (250 µg mL^{-1} for S1-IgG, S1-IgM and CRP, or 50X dilution for NP, in 0.01 M phosphate-buffered saline (PBS, pH 7.4)) and incubated for 3 hours at room temperature, followed by 90 minutes blocking step with 2.0% BSA prepared in 0.01 M PBS. Subsequently, 10 µL of the corresponding target analyte prepared in 0.01 M PBS containing 1.0% BSA was incubated for 1- or 10 minutes at room temperature and, after one washing step with PBS, corresponding detector antibody (HRP labeled or unlabeled) (250X dilution for NP, 2.0 µg mL^{-1} for S1-IgG and S1-IgM, and 1.0 µg mL^{-1} for CRP) in 0.01 M PBS containing 1.0% BSA was incubated for 5 minutes at room temperature. In the case of NP assay, after incubating detector antibody and performing corresponding washing step with PBS, 10 µL of 1.0 µg mL^{-1} HRP-goat anti rabbit IgG prepared in 0.01 M PBS containing 1.0% BSA was incubated for 5 minutes at room temperature. For each type of developed assay, amperometric readings were registered at -0.2 V (*vs.* Ag/AgCl) in 0.05 M sodium phosphate buffer (pH 6.0) containing 2.0 mM HQ. The readout signal was obtained in presence of 1.0 mM H_2O_2.

To characterize the morphology and material properties before and after surface modification with PBA, SEM images of graphene electrodes were obtained by focused ion beam SEM (FIB–SEM, FEI Nova 600 NanoLab).

Electrochemical Characterization of the SARS-CoV-2 RapidPlex

Amperometry, open circuit potential-electrochemical impedance spectroscopy (OCP-EIS), cyclic voltammetry (CV), and differential pulse voltammetry (DPV) were carried out on a CHI820 electrochemical station. The electrochemical setup comprised laser-induced graphene electrodes (LGEs) as the working electrodes (WEs), a platinum wire as the counter electrode (CE), and a commercial Ag/AgCl electrode as the reference electrode (RE).

For each type of proposed assay, surface modification after each step was electrochemically characterized by DPV and OCP-EIS. Corresponding readings by means of each technique

were carried out in 0.01 M PBS (pH 7.4) containing 2.0 mM of $K_4Fe(CN)_6/K_3Fe(CN)_6$ (1:1) and under the following detailed conditions: potential range, -0.2 and 0.6 V; pulse width, 0.2 s; incremental potential, 4 mV; amplitude, 50 mV; frequency range, 0.1–106 Hz; amplitude, 5 mV. Graphene functionalization methods were evaluated for both CRP and SARS-CoV-2 specific IgG assays, by comparing current responses obtained after developing each assay on both PBA and PPA-graphene, in the absence and in the presence of each of the corresponding target biomolecules (tested levels were 50 ng mL^{-1} for CRP and 500 ng mL^{-1} for SARS-CoV-2 specific IgG). Selectivity study was carried out by incubating corresponding interferential non-target molecules on the previously functionalized PBA-graphene. Concentration levels assayed for each interferent were the same as (or even higher than) the concentration of the target molecule in each case. Amperometric signals obtained for each interferent tested were compared to the current signals obtained in the absence and in the presence of the corresponding target analyte for each type of assay.

Design and Fabrication of Electronic System for the SARS-CoV-2 RapidPlex

The 4 channel chronoamperometric measurements were performed by a custom PCB-based wireless potentiostat. An Arm Cortex-M4 microcontroller (STM32L432KC; STMicroelectronics), and a Bluetooth module (SPBT3.0DP2; STMicroelectronics) were used for potentiostat control and wireless communication. A single operational amplifier (AD8605; Analog Devices) was used as the control amplifier, and a quad operational amplifier (AD8608; Analog Devices) was used as a four transimpedance amplifier to construct the potentiostat loop. A series voltage reference (ISL60002; Renesas Electronics) and the MCU's built-in digital to analog converter (DAC) were used to generate the voltage bias across the reference and working electrodes. 4 MCU built-in analog-to-digital converter (ADC) channels were used to concurrently acquire the measurements.

Subjects and Procedures

In compliance with the protocols approved by the Institutional Review Board (no. 19-089417-292-A2) at the California Institute of Technology (Caltech), the performance of SARS-CoV-2 RapidPlex was evaluated in human serum and saliva samples from healthy and confirmed COVID-19 infected patients. Serum samples from 10 RT-PCR and IgG/IgM serology confirmed COVID-19 patients (age range 24-77 years) and 7 healthy subjects (age range 18-65 years) were purchased from BioIVT and Ray Biotech. The severity information of the BioIVT samples was provided by the phlebotomists during sample collection. Saliva

samples from 5 RT-PCR and IgG/IgM serology test confirmed COVID-19 patients (age range 28-46 years) were purchased from BioIVT. 3 healthy saliva samples were used from preexisting stocks collected from volunteers prior to the pandemic (recommended tips before saliva collection include avoiding foods with high sugar and caffeine content, not eating a major meal within 60 minutes of sample collection, and rinsing the mouth with water prior sample collection). After receiving, serum and saliva samples were stored at -80 ºC until required for its analysis. To perform the analysis of NP, CRP, S1-IgG and S1-IgM, no sample treatment was required for both serum and saliva samples; a simple dilution with 0.01 M PBS containing 1.0% BSA was performed prior to analysis.

Determination of SARS-CoV-2 Related Selected Targets Molecules in Serum and Saliva Samples

NP antigen, CRP, and S1-IgG and S1-IgM isotypes were analyzed in commercial serum and saliva samples from RT-PCR COVID-19 confirmed positive patients (n_{serum}=10; n_{saliva}=5) and healthy subjects (n_{serum}=7; n_{saliva}=3). After 100- and 5X dilution of corresponding serum and saliva samples in PBS with 1.0% BSA, respectively, 10 µL-aliquot was incubated in each WE for 10 minutes at room temperature (25X dilution was used for 1-minute incubation study in serum for **Figure 5C**). After washing step with PBS buffer, corresponding detector reagents were incubated in each WE for 5 minutes and subsequent detection was performed. Comparison of sensor performance in buffer and diluted body fluids from healthy subjects spiked with increasing concentrations of target molecule was performed using CRP as a model molecule.

Validation of Human Samples with the Gold Standard ELISA

ELISA tests for NP, S1-IgG and CRP (selected as model targets) were performed in an accuSkan FC Filter-Based Microplate Photometer at a detection wavelength of 450 nm according to the manufacturer's instructions. In brief, plates were coated for 3 hours, shaking at 37 ℃, with 4.0 µg mL^{-1} of the corresponding capture receptor in each case and blocked with PBS containing 1.0% BSA for 2 hours, shaking at 37℃, standards (or properly diluted samples), were added to coated microtiter plate wells and incubated for 2 hours, shaking at 37℃. Next, corresponding HRP-labeled detector antibody was incubated for 30 minutes at room temperature. Finally, 100 µL of 3,3',5,5'-tetramethylbenzidine (TMB) substrate was incubated for 15 minutes, and absorbance values were measured immediately after addition

of 25 µL of 1 M H_2SO_4 in each well. Three washings with PBS containing 1.0% BSA were performed after each modification step.

ACKNOWLEDGEMENTS

This project was supported by the Merkin Institute for Translational Research at Caltech, Emergency COVID-19 Research Seed Funding and COVID-19 Continuation Funding from Tobacco Related-Disease Research Program (TRDRP), TRDRP High Impact Pilot Research Award, National Institute of Health (5R21NR018271), and the Translational Research Institute through NASA NNX16AO69A. J.T. was supported by the National Science Scholarship (NSS) from the Agency of Science Technology and Research (A*STAR) Singapore. We gratefully acknowledge critical support and infrastructure provided for this work by the Kavli Nanoscience Institute at Caltech.

AUTHOR CONTRIBUTIONS

W.G., R.M.T.R., and H.L. initiated the concept and designed the experiments; R.M.T.R., H.L., and J. Tu led the experiments and collected the overall data; Y.Y. performed electrode fabrication and characterization; J.M. performed the circuit design and platform test; C. X. contributed to sensor characterization; W.G., R.M.T.R., and H.L. contributed the data analysis and co-wrote the paper. All authors provided the feedback on the manuscript.

DECLARATION OF INTERESTS

The authors declare no competing interests.

REFERENCES

1. COVID-19 Map - Johns Hopkins Coronavirus Resource Center https://coronavirus.jhu.edu/map.html.
2. Zand, M., and Wang, J. (2020). Potential Mechanisms of Age Related Severity of COVID-19 Infection: Implications for Development of Vaccines, Convalescent Serum, and Antibody Therapies.
3. Anderson, R.M., Heesterbeek, H., Klinkenberg, D., and Hollingsworth, T.D. (2020). How will country-based mitigation measures influence the course of the COVID-19 epidemic? The Lancet *395*, 931–934.
4. Prager, F., Wei, D., and Rose, A. (2017). Total Economic Consequences of an Influenza Outbreak in the United States. Risk Anal. *37*, 4–19.

5. Park, S.W., Cornforth, D.M., Dushoff, J., and Weitz, J.S. (2020). The time scale of asymptomatic transmission affects estimates of epidemic potential in the COVID-19 outbreak. Epidemics *31*, 1–18.
6. Li, Q., Guan, X., Wu, P., Wang, X., Zhou, L., Tong, Y., Ren, R., Leung, K.S.M., Lau, E.H.Y., Wong, J.Y., et al. (2020). Early transmission dynamics in Wuhan, China, of novel coronavirus-infected pneumonia. N. Engl. J. Med. *382*, 1199–1207.
7. Mizumoto, K., Kagaya, K., Zarebski, A., and Chowell, G. (2020). Estimating the asymptomatic proportion of coronavirus disease 2019 (COVID-19) cases on board the Diamond Princess cruise ship, Yokohama, Japan, 2020. Eurosurveillance *25*, 1–5.
8. Nishiura, H., Kobayashi, T., Miyama, T., Suzuki, A., Jung, S., Hayashi, K., Kinoshita, R., Yang, Y., Yuan, B., Akhmetzhanov, A.R., et al. (2020). International Journal of Infectious Diseases. Int. J. Infect. Dis. *94*, 154–155.
9. Li, Z., Yi, Y., Luo, X., Xiong, N., Liu, Y., Li, S., Sun, R., Wang, Y., Hu, B., Chen, W., et al. (2020). Development and clinical application of a rapid IgM-IgG combined antibody test for SARS-CoV-2 infection diagnosis. J. Med. Virol. *92*, 1518–1524.
10. 'It's Like Having No Testing': Coronavirus Test Results Are Still Delayed - The New York Times https://www.nytimes.com/2020/08/04/us/virus-testing-delays.html.
11. ID NOW COVID-19 | Rapid point of care diagnostics – Abbott https://www.globalpointofcare.abbott/en/product-details/id-now-covid-19.html.
12. van Dongen, J.E., Berendsen, J.T.W., Steenbergen, R.D.M., Wolthuis, R.M.F., Eijkel, J.C.T., and Segerink, L.I. (2020). Point-of-care CRISPR/Cas nucleic acid detection: Recent advances, challenges and opportunities. Biosens. Bioelectron. *166*, 112445.
13. Huang, Z., Tian, D., Liu, Y., Lin, Z., Lyon, C.J., Lai, W., Fusco, D., Drouin, A., Yin, X., Hu, T., et al. (2020). Ultra-sensitive and high-throughput CRISPR-p owered COVID-19 diagnosis. Biosens. Bioelectron. *164*, 112316.
14. Guo, L., Sun, X., Wang, X., Liang, C., Jiang, H., Gao, Q., Dai, M., Qu, B., Fang, S., Mao, Y., et al. (2020). SARS-CoV-2 detection with CRISPR diagnostics. Cell Discov. *6*, 4–7.
15. Kellner, M.J., Koob, J.G., Gootenberg, J.S., Abudayyeh, O.O., and Zhang, F. (2019). SHERLOCK: nucleic acid detection with CRISPR nucleases. Nat. Protoc. *14*, 2986–3012.
16. Yang, Y., Yang, M., Shen, C., Wang, F., Yuan, J., Li, J., Zhang, M., Wang, Z., Xing, L., Wei, J., et al. (2020). Evaluating the accuracy of different respiratory specimens in the laboratory diagnosis and monitoring the viral shedding of 2019-nCoV infections. medRxiv. 10.1101/2020.02.11.20021493.

17. Sethuraman, N., Jeremiah, S. S., Ryo, A. (2020) Interpreting Diagnostic Tests for SARS-CoV-2. JAMA *323*, 2249–2251.
18. Lisboa Bastos, M., Tavaziva, G., Abidi, S.K., Campbell, J.R., Haraoui, L.P., Johnston, J.C., Lan, Z., Law, S., MacLean, E., Trajman, A., et al. (2020). Diagnostic accuracy of serological tests for covid-19: Systematic review and meta-analysis. BMJ *370*, m2516.
19. Gong, J., Dong, H., Xia, S.Q., Huang, Y.Z., Wang, D., Zhao, Y., Liu, W., Tu, S., Zhang, M., Wang, Q., et al. (2020) Correlation Analysis Between Disease Severity and Inflammation-related Parameters in Patients with COVID-19 Pneumonia, medRxiv. 10.1101/2020.02.25.20025643.
20. Wu, C., Chen, X., Cai, Y., Xia, J., Zhou, X., Xu, S., Huang, H., Zhang, L., Zhou, X., Du, C., et al. (2020). Risk Factors Associated with Acute Respiratory Distress Syndrome and Death in Patients with Coronavirus Disease 2019 Pneumonia in Wuhan, China. JAMA Intern. Med. *180*, 934–943.
21. Zhou, B. (2019). Utility of Ferritin , Procalcitonin , and C-reactive Protein in Severe Patients with 2019 Novel Coronavirus Disease. 10.21203/rs.3.rs-18079/v1.
22. Morales-Narváez, E., and Dincer, C. (2020). The impact of biosensing in a pandemic outbreak: COVID-19. Biosens. Bioelectron. *163*, 112274.
23. Jalandra, R., Yadav, A.K., Verma, D., Dalal, N., Sharma, M., Singh, R., Kumar, A., and Solanki, P.R. (2020). Strategies and perspectives to develop SARS-CoV-2 detection methods and diagnostics. Biomed. Pharmacother. *129*, 110446.
24. Seo, G., Lee, G., Kim, M.J., Baek, S.H., Choi, M., Ku, K.B., Lee, C.S., Jun, S., Park, D., Kim, H.G., et al. (2020). Rapid Detection of COVID-19 Causative Virus (SARS-CoV-2) in Human Nasopharyngeal Swab Specimens Using Field-Effect Transistor-Based Biosensor. ACS Nano *14*, 5135–5142.
25. Chandra, P. (2020). Miniaturized Label-free Smartphone Assisted Electrochemical Sensing Approach for Personalized COVID-19 Diagnosis. Sens. Int. *1*, 100019.
26. Mahari, S., Roberts, A., Shahdeo, D., and Gandhi, S. (2020). eCovSens-Ultrasensitive Novel In-House Built Printed Circuit Board Based Electrochemical Device for Rapid Detection of nCovid-19. bioRxiv. 10.1101/2020.04.24.059204.
27. Tripathy, S., and Singh, S.G. (2020). Label-Free Electrochemical Detection of DNA Hybridization: A Method for COVID-19 Diagnosis. Trans. Indian Natl. Acad. Eng. 10.1007/s41403-020-00103-z.
28. Pasomsub, E., Watcharananan, S.P., Boonyawat, K., Janchompoo, P., Wongtabtim, G., Suksuwan, W., Sungkanuparph, S., and Phuphuakrat, A. (2020). Saliva sample as a non-

invasive specimen for the diagnosis of coronavirus disease 2019 : a cross-sectional study. medRxiv. 10.1101/2020.04.17.20070045.

29. Yang, Y., Song, Y., Bo, X., Min, J., Pak, O.S., Zhu, L., Wang, M., Tu, J., Kogan, A., Zhang, H., et al. (2020). A laser-engraved wearable sensor for sensitive detection of uric acid and tyrosine in sweat. Nat. Biotechnol. *38*, 217–224.
30. Torrente-Rodríguez, R.M., Tu, J., Yang, Y., Min, J., Wang, M., Song, Y., Yu, Y., Xu, C., Ye, C., IsHak, W.W., et al. (2020). Investigation of Cortisol Dynamics in Human Sweat Using a Graphene-Based Wireless mHealth System. Matter *2*, 921–937.
31. Diao, B., Wen, K., Chen, J., Liu, Y., Yuan, Z., Han, C., Chen, J., Pan, Y., Chen, L., Dan, Y., et al. (2020). Diagnosis of Acute Respiratory Syndrome Coronavirus 2 Infection by Detection of Nucleocapsid Protein. medRxiv. 10.1101/2020.03.07.20032524.
32. Hinnemo, M., Zhao, J., Ahlberg, P., Hägglund, C., Djurberg, V., Scheicher, R.H., Zhang, S.L., and Zhang, Z. Bin (2017). On Monolayer Formation of Pyrenebutyric Acid on Graphene. Langmuir *33*, 3588–3593.
33. Gao, F., Zhang, X., Gao, F., Cai, X., Zheng, M., Jiang, S., and Wang, Q. (2013). Application of graphene-pyrenebutyric acid nanocomposite as probe oligonucleotide immobilization platform in a DNA biosensor. Mater. Sci. Eng. C *33*, 3851–3857.
34. Yi, E., Teo, L., Yusoff, M.M., and Chong, K.F. (2015). ICGSCE 2014, 185–193.
35. Karachevtsev, V.A., Stepanian, S.G., Glamazda, A.Y., Karachevtsev, M. V., Eremenko, V. V., Lytvyn, O.S., and Adamowicz, L. (2011). Noncovalent interaction of single-walled carbon nanotubes with 1-pyrenebutanoic acid succinimide ester and glucoseoxidase. J. Phys. Chem. C *115*, 21072–21082.
36. Fernandes, E., Cabral, P.D., Campos, R., Machado, G., Cerqueira, M.F., Sousa, C., Freitas, P.P., Borme, J., and Petrovykh, D.Y. (2020). Functionalization of single-layer graphene for immunoassays. Appl. Surf. Sci. *480*, 709–716.
37. Ericsson, E.M., Enander, K., Bui, L., Lundström, I., Konradsson, P., and Liedberg, B. (2013). Site-specific and covalent attachment of his-tagged proteins by chelation assisted photoimmobilization: A strategy for microarraying of protein ligands. Langmuir *29*, 11687–11694.
38. Dobaño, C., Vidal, M., Santano, R., Jiménez, A., Chi, J., Barrios, D., Ruiz-Olalla, G., Melero, N.R., Carolis, C., Parras, D., et al. (2020). Highly sensitive and specific multiplex antibody assays to quantify immunoglobulins M, A and G against SARS-CoV-2 antigens. 10.1101/2020.06.11.147363

39. Qian, C., Zhou, M., Cheng, F., Lin, X., Gong, Y., Xie, X., Li, P., Li, Z., Zhang, P., Liu, Z., et al. (2020). Development and multicenter performance evaluation of fully automated SARS-CoV-2 IgM and IgG immunoassays. Clin. Chem. Lab. Med. *58*, 1601–1607.
40. Ma, H., Zeng, W., He, H., Zhao, D., Yang, Y., Jiang, D., Zhou, P., Qi, Y., He, W., Zhao, C., et al. (2020). COVID-19 diagnosis and study of serum SARS-CoV-2 specific IgA, IgM and IgG by a quantitative and sensitive immunoassay. medRxiv. 10.1101/2020.04.17.20064907.
41. Ni, L., Ye, F., Cheng, M.L., Feng, Y., Deng, Y.Q., Zhao, H., Wei, P., Ge, J., Gou, M., Li, X., et al. (2020). Detection of SARS-CoV-2-Specific Humoral and Cellular Immunity in COVID-19 Convalescent Individuals. Immunity *52*, 971-977.e3.
42. Zhao, R., Li, M., Song, H., Chen, J., Ren, W., Feng, Y., Gao, G.F., Song, J., Peng, Y., Su, B., et al. (2020). Early detection of SARS-CoV-2 antibodies in COVID-19 patients as a serologic marker of infection. Clin. Infect. Dis. ciaa523.
43. Zhao J, Yuan Q, Wang H, et al. (2020). Antibody responses to SARS-CoV-2 in patients of novel coronavirus disease 2019. Clin Infect Dis. ciaa344.
44. Nicol, T., Lefeuvre, C., Serri, O., Pivert, A., Joubaud, F., Dubée, V., Kouatchet, A., Ducancelle, A., Lunel-Fabiani, F., and Le Guillou-Guillemette, H. (2020). Assessment of SARS-CoV-2 serological tests for the diagnosis of COVID-19 through the evaluation of three immunoassays: Two automated immunoassays (Euroimmun and Abbott) and one rapid lateral flow immunoassay (NG Biotech). J. Clin. Virol. *129*, 104511.
45. Ai, T., Yang, Z., Hou, H., Zhan, C., Chen, C., Lv, W., Tao, Q., Sun, Z., and Xia, L. (2020). Correlation of Chest CT and RT-PCR Testing in Coronavirus Disease 2019 (COVID-19) in China: A Report of 1014 Cases. Radiology *2019*, 200642.
46. Chan, J.F.W., Yip, C.C.Y., To, K.K.W., Tang, T.H.C., Wong, S.C.Y., Leung, K.H., Fung, A.Y.F., Ng, A.C.K., Zou, Z., Tsoi, H.W., et al. (2020). Improved molecular diagnosis of COVID-19 by the novel, highly sensitive and specific COVID-19-RdRp/Hel real-time reverse transcription-PCR assay validated in vitro and with clinical specimens. J. Clin. Microbiol. *58*, e00310–20.
47. Yip, C.C.Y., Ho, C.C., Chan, J.F.W., To, K.K.W., Chan, H.S.Y., Wong, S.C.Y., Leung, K.H., Fung, A.Y.F., Ng, A.C.K., Zou, Z., et al. (2020). Development of a novel, genome subtraction-derived, sars-cov-2-specific covid-19-nsp2 real-time rt-pcr assay and its evaluation using clinical specimens. Int. J. Mol. Sci. *21*, 1–11.

48. Zhang, Y., Odiwuor, N., Xiong, J., Sun, L., Nyaruaba, R.O., Wei, H., and Tanner, N.A. (2020). Rapid Molecular Detection of SARS-CoV-2 (COVID-19) Virus RNA Using Colorimetric LAMP. medRxiv. 10.1101/2020.02.26.20028373.
49. Teng, F., Guo, L., Cui, T., Wang, X.G., Xu, K., Gao, Q., Zhou, Q., and Li, W. (2019). CDetection: CRISPR-Cas12b-based DNA detection with sub-attomolar sensitivity and single-base specificity. Genome Biol. *20*, 1–7.
50. Nachtigall, F.M., Pereira, A., Trofymchuk, O.S., and Santos, L.S. Detection of SARS-CoV-2 in nasal swabs using. Nat. Biotechnol. 10.1038/s41587-020-0644-7.
51. Wang, P. (2020). Combination of serological total antibody and RT-PCR test for detection of SARS-COV-2 infections. J. Virol. Methods *283*, 113919.
52. Carvalho, A.M.R.S., De Oliveira Mendes, T.A., Coelho, E.A.F., Duarte, M.C., and Menezes-Souza, D. (2018). New antigens for the serological diagnosis of human visceral leishmaniasis identified by immunogenomic screening. PLoS ONE *13*, 1–16.
53. Alizadeh, S.A., Abdolahpour, G., Pourmand, M., Naserpour, T., Najafipour, R., and Eshraghi, S.S. (2014). Evaluation of New ELISA based on rLsa63 - rLipL32 antigens for serodiagnosis of Human Leptospirosis. Iran. J. Microbiol. *6*, 184–189.
54. Feng, W., Newbigging, A., Le, C., Pang, B., Peng, H., Cao, Y., Wu, J., Abbas, G., Song, J., Wang, D.-B., et al. (2020). Molecular diagnosis of COVID-19: Challenges and research needs. Anal. Chem. *92*, 10196–10209.
55. Grifoni, A., Sidney, J., Zhang, Y., Scheuermann, R.H., Peters, B., and Sette, A. (2020). A Sequence Homology and Bioinformatic Approach Can Predict Candidate Targets for Immune Responses to SARS-CoV-2. Cell Host Microbe *27*, 671-680.e2.
56. Kannan, S., Subbaram, K., Ali, S., and Kannan, H. (2020). Molecular characterization and amino acid homology of nucleocapsid (N) Protein in SARS-CoV-1, SARS-CoV-2, MERS-CoV, and bat coronavirus. J. Pure Appl. Microbiol. *14*, 757–763.
57. Liu, F., Li, L., Xu, M., Wu, J., Luo, D., Zhu, Y., Li, B., and Song, X. (2020). Prognostic value of interleukin-6 , C-reactive protein , and procalcitonin in patients with COVID-19. J. Clin. Virol. *127*, 104370.
58. Huang, I., Pranata, R., Lim, M.A., Oehadian, A., and Alisjahbana, B. (2020). C-reactive protein, procalcitonin, D-dimer, and ferritin in severe coronavirus disease-2019: a meta-analysis. Ther. Adv. Respir. Dis. *14*, 1–14.
59. Sun, Y., Dong, Y., Wang, L., Xie, H., Li, B., Chang, C., and Wang, F. sheng (2020). Characteristics and prognostic factors of disease severity in patients with COVID-19: The Beijing experience. J. Autoimmun. *112*, 102473.

60. Shang, W., Dong, J., Ren, Y., Tian, M., Li, W., Hu, J., and Li, Y. (2020). The value of clinical parameters in predicting the severity of COVID-19. J. Med. Virol. *92*, 2188–2192.
61. Tan, C., Huang, Y., Shi, F., Tan, K., Ma, Q., Chen, Y., Jiang, X., and Li, X. (2020). C-reactive protein correlates with computed tomographic findings and predicts severe COVID-19 early. J. Med. Virol. *92*, 856–862.
62. Chen, W., Zheng, K.I., Liu, S., Yan, Z., Xu, C., and Qiao, Z. (2020). Plasma CRP level is positively associated with the severity of COVID-19. Ann. Clin. Microbiol. Antimicrob. *19*, 1–7.
63. Xu, C., Yang, Y., and Gao, W. (2020). Skin-Interfaced Sensors in Digital Medicine : from Materials to Applications. Matter *2*, 1414–1445.
64. Yang, Y., and Gao, W. (2019). Wearable and flexible electronics for continuous molecular monitoring. Chem. Soc. Rev. *48*, 1465–1491.
65. Adans-dester, C.P., Bamberg, S., Bertacchi, F.P., Caulfield, B., Chappie, K., Demarchi, D., Erb, M.K., Estrada, J., Fabara, E.E., Freni, M., et al. (2020). Can mHealth Technology Help Mitigate the Effects of the COVID-19 Pandemic? IEEE Eng. Med. Biol. *1*, 242–248.
66. Jeong, H., Adv, S., Jeong, H., Rogers, J.A., and Xu, S. (2020). Continuous on-body sensing for the COVID-19 pandemic : Gaps and opportunities. Sci. Adv. *6*, eabd4794.
67. Kim, J., Campbell, A.S., Ávila, B.E. De, and Wang, J. (2019). Wearable biosensors for healthcare monitoring. Nat. Biotechnol. *37*, 389–406.

FIGURE CAPTIONS

Figure 1. A Wireless Graphene-based Telemedicine Platform (SARS-CoV-2 RapidPlex) for Rapid and Multiplex Electrochemical Detection of SARS-CoV-2 in Blood and Saliva.

(A) Schematic illustration of the SARS-CoV-2 RapidPlex multisensor telemedicine platform for detection of SARS-CoV-2 viral proteins, antibodies (IgG and IgM), and inflammatory biomarker – C-reactive protein (CRP). Data can be wirelessly transmitted to a mobile user interface. WE, working electrode; CE, counter electrode; RE, reference electrode.

(B) Mass-producible laser-engraved graphene sensor arrays.

(C) Photograph of a disposable and flexible graphene array.

(D) Image of a SARS-CoV-2 RapidPlex system with a graphene sensor array connected to a printed circuit board for signal processing and wireless communication.

Figure 2. Characterization of Electrochemical Graphene Biosensors Comprising the SARS-CoV-2 RapidPlex Platform.

(A) Scheme detailing the methodology developed for the covalent attachment of the corresponding bioreceptor for the specific capture of the target analytes SARS-CoV-2 NP and CRP (left), and IgG and IgM isotypes against SARS-CoV-2 S1 protein (right). PBA, 1-Pyrenebutyric acid; BSA, bovine serum albumin; CAb, capture antibody; PI, polyimide.

(B) and (C) Differential pulse voltammetry (DPV) and Nyquist plots of a graphene electrode in 0.01 M phosphate-buffered saline (PBS, pH 7.4) containing 2.0 mM of $K_4Fe(CN)_6/K_3Fe(CN)_6$ (1:1) after each modification step (S1-IgG assay as representative example): bare graphene (Bare), functionalization with PBA (PBA), immobilization of SARS-CoV-2 S1 protein (Protein), blocking with BSA (BSA), recognition of specific S1-IgG (Target), and incubation with enzyme-tagged anti-human IgG antibody (DAb).

(D) Comparison of amperometric responses and overlaid signal-to-blank (S/B) ratio (black lines) for SARS-CoV-2 specific IgG and CRP detection using PBA and 1H-pyrrole-1-propionic acid (PPA) as linkers for the attachment of the corresponding capture bioreceptors. Data are presented as mean ± SD (n = 3).

(E) Amperometric responses and overlaid S/B ratio (black lines) observed for 0.0 and 500 pg mL^{-1} NP, 0.0 and 250 ng mL^{-1} SARS-CoV-2 specific IgG and IgM, and 0.0 and 50 ng mL^{-1} CRP, with 10, 5 and 1-minute incubation. Data are presented as mean ± SD (n = 3).

Figure 3. Evaluation of Analytical Sensor Performance for the Detection of Physiological Levels of Target COVID-19 Biomarkers.

(A) Scheme of sensor preparation for detection of SARS-CoV-2 NP and CRP based on double-sandwich and sandwich assay configurations, respectively. CAb, capture antibody; DAb, detector antibody; DAb_2, secondary detector antibody; HRP, horseradish peroxidase.

(B) and (C) Calibration curves constructed for NP (B) and CRP (C) detection in phosphate-buffered saline (PBS, pH 7.4) supplemented with 1.0% BSA. Data are presented as mean ± SD (n = 3).

(D) Scheme of sensor preparation for detection of S1- IgG and S1-IgM isotypes based on direct assay configurations.

(E) and (F) Calibration curves constructed for S1-IgG (E) and S1-IgM (F) isotypes detection in phosphate-buffered saline (PBS, pH 7.4) supplemented with 1.0% BSA. Data are presented as mean ± SD (n = 3).

Figure 4. Investigation of the Selectivity and Multiplexed Performance of the Wireless SARS-CoV-2 RapidPlex Platform.

(A) Selective response of NP, S1-IgG and S1-IgM isotypes and CRP sensors against different non-target circulating analytes. Interferential molecules were tested at 500 pg mL^{-1} (with an exception of 50 ng mL^{-1} for CRP), 250 ng mL^{-1} and 50 ng mL^{-1} for NP, S1-IgG and S1-IgM, and CRP assays, respectively. Data are presented as mean ± SD (n = 3).

(B) Validation of sample concentrations measured using the designed electrochemical sensor against sample concentrations measured using ELISA.

(C) Block diagram of the SARS-CoV-2 RapidPlex platform. UART, universal asynchronous receiver/transmitter; MCU, microcontroller unit; DAC, digital-to-analog converter; ADC, analog-to-digital converter.

(D) Schematic illustration of the graphene sensor array layout.

(E) Experimental readings obtained with the functionalized SARS-CoV-2 RapidPlex platform after incubation of the four WEs with phosphate-buffered saline (PBS, pH 7.4) supplemented with 1.0% BSA containing 1.0 ng mL^{-1} NP (I), 250 ng mL^{-1} S1-IgG (II), 250 ng mL^{-1} S1-IgM (III) and 50 ng mL^{-1} CRP (IV).

Figure 5. Application of SARS-CoV-2 RapidPlex in SARS-CoV-2 Detection in Blood and Saliva Samples from COVID-19 Positive and Negative subjects.

(A and B) Experimental readings obtained with SARS-CoV-2 RapidPlex after 10 minutes incubation of the sensor array with serum samples from a representative COVID-19 RT-PCR negative (A) and positive patient (B).

(C) The signal of individual sensor obtained after 1-minute incubation with a serum sample from a COVID-19 positive patient (dark color) *vs.* the signal obtained after 10-minute incubation with a serum sample from a COVID-19 negative patient (light color).

(D) A box-and-whisker plot of measured signal-to-blank ratios (S/B) for NP, S1-IgG, S1-IgM, and CRP in RT-PCR confirmed COVID-19 positive (n=5) and negative (n=6) serum samples.

(E) A box-and-whisker plot of measured signal-to-blank ratios (S/B) for NP, S1-IgG, S1-IgM, and CRP in RT-PCR confirmed COVID-19 positive (n=5) and negative (n=3) saliva samples.

(F) CRP levels in diluted serum samples plotted against given COVID-19 symptom severity, with “Healthy” referring to COVID-19 negative patient samples (n=7). Positive COVID-19 patients classified according to disease severity as asymptomatic (n=2), mild (n=5) and moderate (n=2).

Table 1. Key Information on an Individual's COVID-19 Infection Status Provided by the SARS-CoV-2 RapidPlex. +, higher than threshold; -, lower than threshold; ||, or.

Viral Antigen	IgM	IgG	CRP	Expected Outcome
-	-	-	-	Healthy
+	+ || -	-	-	Infectious, Presymptomatic
+	+ || +		-	Infectious, Asymptomatic
+	+ || +		+	Infectious, Symptomatic
-	+	+ || -	+ || -	Recovered (recently)
-	-	+	-	Recovered (long term)
-	-	-	+	Inflammation/infection not due to COVID-19

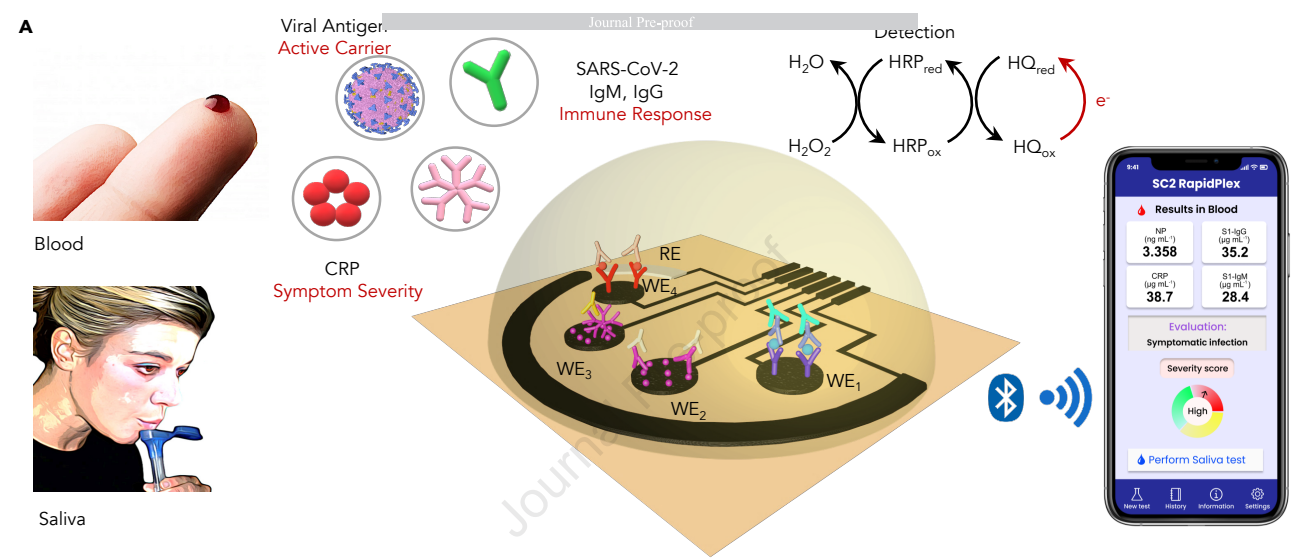

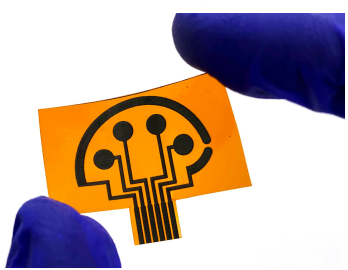

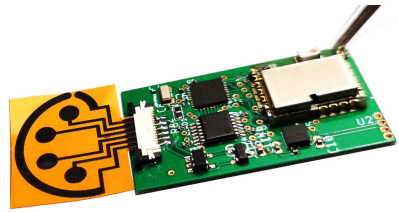

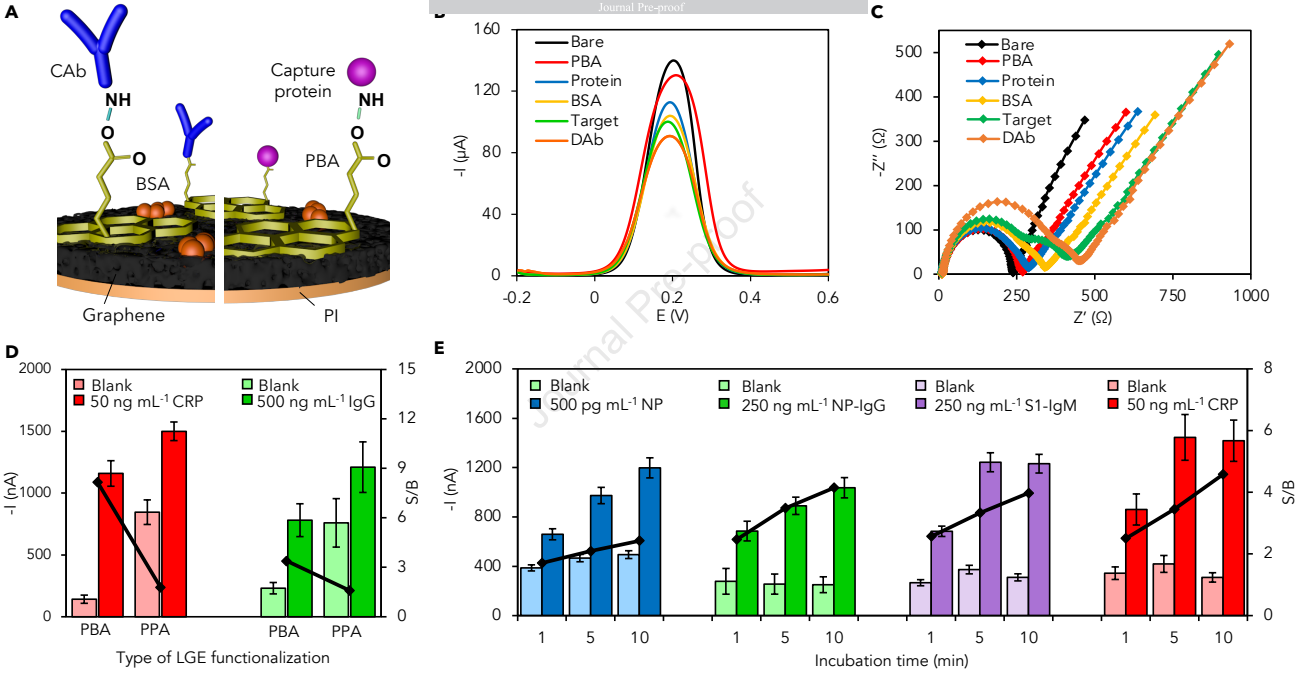

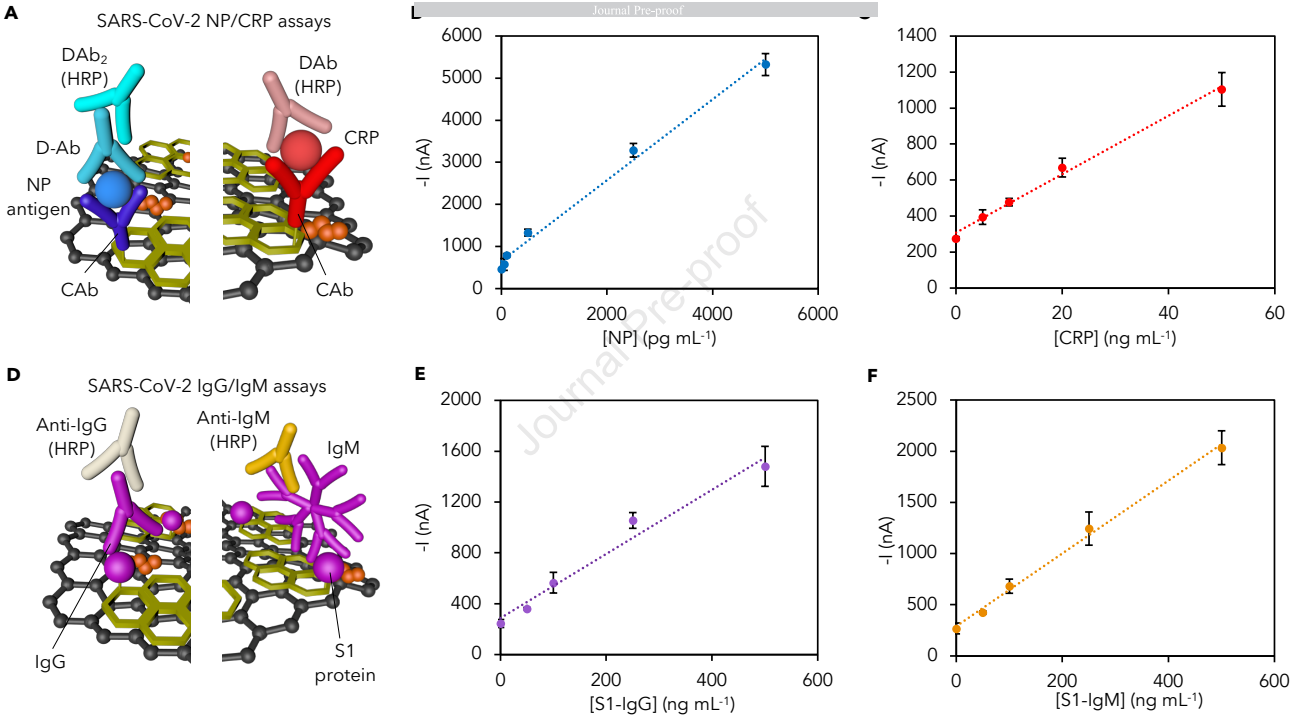

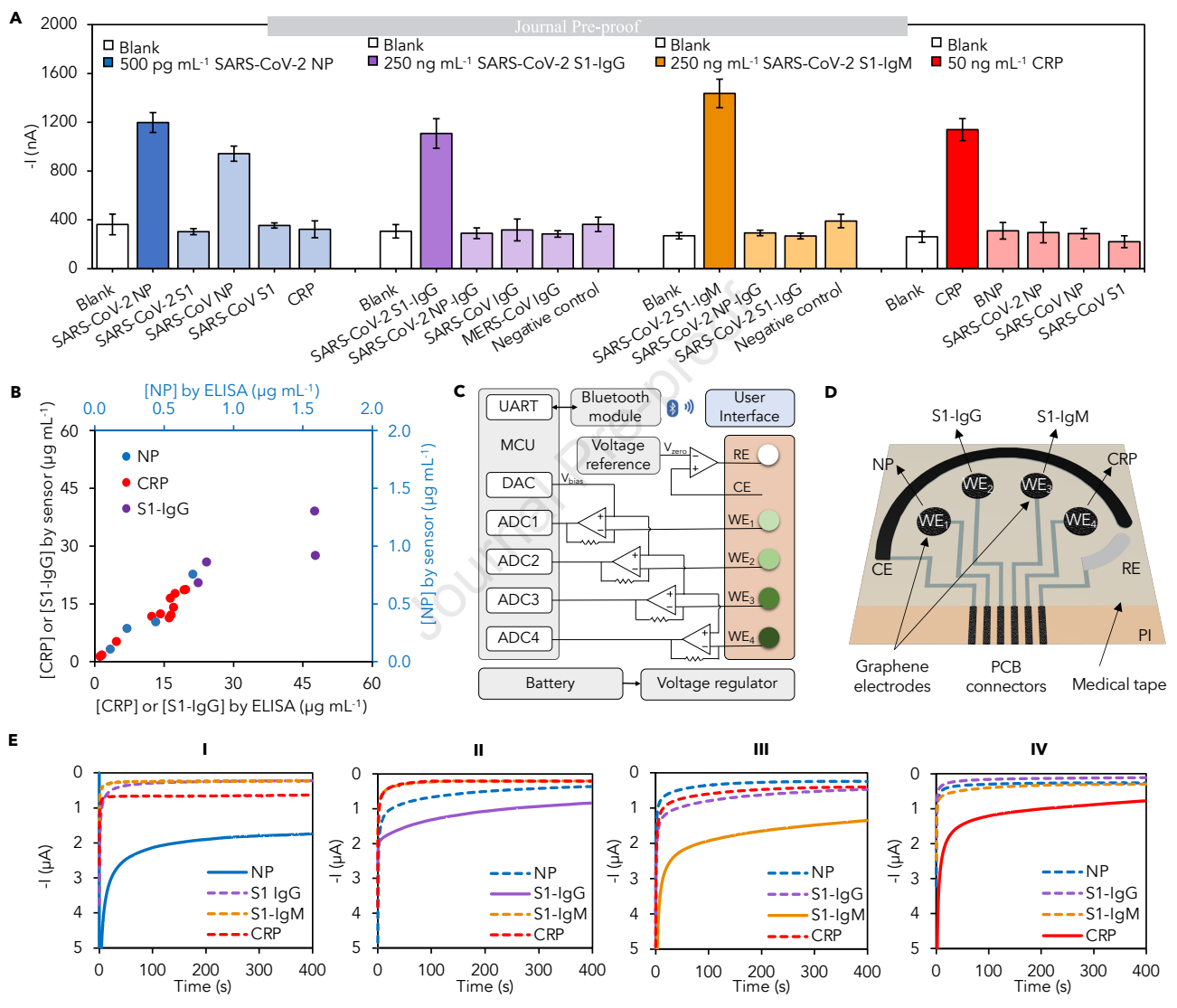

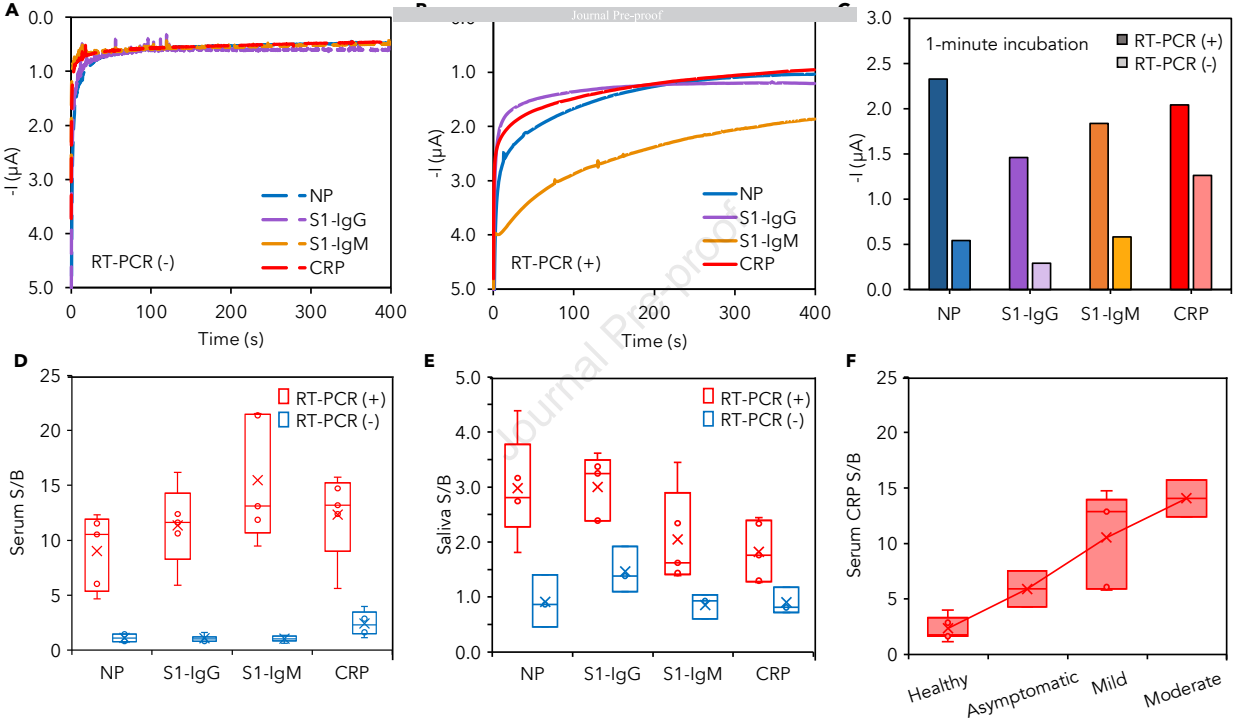

Progress and Potential

The need for widespread testing to control the spread of COVID-19 has faced challenges due to testing backlogs, limited access to required equipment, and inaccurate assay results. To address this, we propose an ultrasensitive and low-cost telemedicine platform – the SARS-CoV-2 RapidPlex – based on target-specific immunoassays built off laser-engraved graphene for rapid and remote assessment of COVID-19 biomarkers (i.e., nucleocapsid protein, anti-spike protein IgG and IgM, and C-reactive protein). Multiplex sensing of these targets provides information on three key aspects of COVID-19 disease: viral infection, immune response, and disease severity. We successfully demonstrated the platform's applicability using COVID-19 positive and negative serum and saliva samples. The SARS-CoV-2 RapidPlex has the potential to quickly and effectively triage patients and track infection progression, allowing for the clear identification of individuals who are infectious, vulnerable, and/or immune.

Highlights

- Multiplexed detection of SARS-CoV-2 antigen, antibodies, and C-reactive protein.
- Low-cost and mass manufacturable platform using laser-engraved graphene.
- Wireless telemedicine sensing platform with rapid sample-to-answer turnaround.
- Successful device evaluation in both COVID-19 patient blood and saliva samples.

e-TOC

The SARS-CoV-2 RapidPlex is developed based on laser-engraved graphene immunosensors to electrochemically quantify SARS-CoV-2 nucleocapsid protein, IgG and IgM, and C-reactive protein (CRP). The platform is characterized by rapid detection, and high molecular sensitivity, selectivity. Pilot study results demonstrate that it can successfully detect these biomarkers in COVID-19 positive patient serum and saliva samples. CRP results are well-correlated with symptom severity, indicating the potential for this integrated system to be used as a diagnostic tool for telemedicine COVID-19 patient care.